Self-Association and Membrane-Binding Behavior of Melittins Containing Trifluoroleucine

Angelika Niemz and David A. Tirrell*

Contribution from the Division of Chemistry and Chemical Engineering, California Institute of Technology, Pasadena, California 91125

Received December 27, 2000

Abstract: We have investigated the effect of trifluoroleucine substitution on the membrane-binding and tetramerization behavior of melittin. Analogues were synthesized in which Leu 9, Leu 13, and all four intrinsic leucine residues of melittin were replaced by 5,5,5-trifluoroleucine. Both the mono- and tetra-substituted melittins were found to exhibit stronger self-association and enhanced affinity for lipid bilayer membranes, compared to the wild-type peptide. The extent of the observed effects depends on the site of introduction of trifluoroleucine and, in the case of substitution at position 13, on the stereochemistry of the trifluoroleucine side chain. Analysis of the membrane association isotherms is consistent with aggregation of fluorinated melittins within the lipid bilayer. These results suggest that fluorocarbon−hydrocarbon separation, in addition to an increase in hydrophobic character, contributes to enhanced membrane binding.

Introduction

Melittin, the major component of bee venom, is a 26 amino acid, amphiphilic peptide, which inserts into membranes and causes cell lysis. It has been intensely studied both as a model for peptides with membrane affinity and to understand the structural bases of its lytic and antimicrobial activities.[1−3]

In aqueous solution at submillimolar concentration and low ionic strength, melittin exists as a random coil monomer, mainly due to repulsive interactions between the highly charged C-terminal regions (Scheme 1A). At higher ionic strength, especially in the presence of divalent anions, melittin forms a water-soluble tetramer with known crystal structure (Scheme 1B).[4,5] Each monomer assumes the conformation of a bent α-helical rod, with three sections showing distinctive spatial segregation of hydrophobic and hydrophilic side chains.[4] Section 1, consisting of amino acid residues 1−6, is entirely hydrophobic except for the positively charged N-terminus. Section 2, which includes amino acid residues 7−20, is amphiphilic, with hydrophobic residues on the inside, and polar residues on the outside of the bent region (with the exception of Pro 14). Section 3 comprises amino acid residues 21−26, is entirely polar, and contains four positively charged side chains.

Insertion into a phospholipid bilayer also causes melittin to adopt a bent helical conformation (Scheme 1C).[6] While the C-terminal section is approximately parallel to the lipid bilayer, the N-terminal section is inserted halfway into the membrane, as confirmed by fluorescence quenching, NMR, ATR-IR, and computational studies.[7,8] The mechanism of cell lysis caused by melittin is still under debate. One model proposes that the wedge-like insertion of melittin monomers into one side of the bilayer disrupts the membrane, causing water penetration and leakage of small molecules.[9] Resonance energy transfer studies suggest that the majority of membrane-bound melittin is monomeric.[10] The "barrel-stave" model, on the other hand, proposes that a fraction of the membrane-bound melittin attains a trans-membrane orientation, followed by oligomerization leading to discrete pores.[11] Support for the barrel-stave model comes from time-resolved efflux measurements and from the observation of melittin-induced, voltage-gated single channel conductivities.[11−13]

Scheme 1. aa-Sequence of Melittin with Hydrophobic (orange) and Polar (blue) Residues: (A) Random Coil Conformation in Equilibrium with the (B) Tetramer and (C) Lipid Bound Monomer[a]

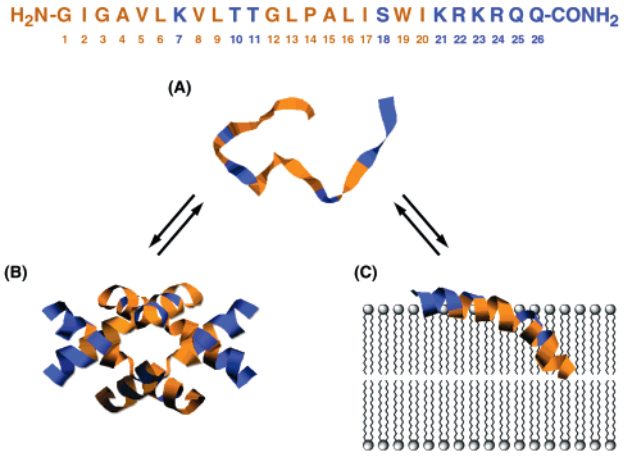

[a] Structures of the melittin tetramer and monomer are according to PDB-entry 2MLT.[5]

(1) Dempsey, C. *Biochim. Biophys. Acta* **1990**, *1031*, 143−161.
(2) Kaiser, E. T.; Kezdy, F. J. *Annu. Rev. Biophys. Biophys. Chem.* **1987**, *16*, 561−581.
(3) Bechinger, B. *J. Membr. Biol.* **1997**, *156*, 197−211.
(4) Terwilliger, T. C.; Weissman, L.; Eisenberg, D. *Biophys. J.* **1982**, *37*, 353−361.
(5) Terwilliger, T. C.; Eisenberg, D. *J. Biol. Chem.* **1982**, *257*, 6016−6022.
(6) Schwarz, G.; Beschiavili, G. *Biochim. Biophys. Acta* **1989**, *979*, 82−90.
(7) Weaver, A. J.; Kemple, M. D.; Brauner, J. W.; Mendelson, R.; Prendergast, F. G. *Biochemistry* **1992**, *31*, 1301−1313.
(8) Berneche, S.; Nina, M.; Roux, B. *Biophys. J.* **1998**, *75*, 1603−1618.
(9) Bachar, M.; Becker, O. *J. Chem. Phys.* **1999**, *111*, 8672−8685.
(10) John, E.; Jaehnig, F. *Biophys. J.* **1991**, *60*, 319−328.

10.1021/ja004351p CCC: $20.00
Published on Web 07/10/2001

Hydrophobic interactions provide the main driving force for tetramerization and membrane-insertion of melittin: apolar side chains are either buried on the inside of the tetramer or inserted into the hydrophobic interior of the membrane, sequestered from the solvent. One approach to increasing the hydrophobic character of organic solutes is to substitute hydrogen with fluorine. Compared to their hydrocarbon analogues, fluorocarbons often exhibit lower aqueous solubility, higher contact angles with water, and greater partition constants between aqueous and organic phases, indicative of enhanced hydrophobicity.[14−16] Fluorine (VdW radius = 1.35 Å) and hydrogen (VdW radius = 1.2 Å) are nearly isosteric, and although the C−F bond is 0.4 Å longer than the C−H bond, fluorination generally causes only modest structural perturbation.[14] Perfluorinated lipids have been used to generate highly stable fluoroliposomes applicable in drug delivery,[17] and fluorination presents a common strategy in drug design to increase hydrophobicity, resulting in enhanced drug bioavailability[18,19] and specificity for lipophilic target enzymes.[20] Fluorination can induce formation of supramolecular structures in the form of microdomains, caused by phase separation between fluorocarbons and hydrocarbons. This has been demonstrated in fluorocarbon/hydrocarbon copolymers,[21] as well as in mixed and partially fluorinated colloidal, micellar, and lipid lamellar systems.[17] In a recent review it was predicted that the hydrophobic and structure-forming properties of fluorocarbons could be exploited in the context of protein engineering through the introduction of fluorinated amino acids, potentially providing proteins and peptides of enhanced tertiary and quarternary structural stability and increased lipophilicity.[22] Indeed, in recent studies we[23,24] and others[25] have shown that introducing 5,5,5-trifluoroleucine into the *d*-positions of leucine-zipper peptides substantially enhances the stability of the coiled-coil dimer toward thermal or chemical denaturation. We were further able to demonstrate that the fluorinated peptides maintain their affinity and specificity of binding to target DNA sequences.[24] We and others have demonstrated that incorporation of fluorine is not restricted to peptides accessible via solid-phase synthesis, since fluorinated analogues of the aromatic amino acids,[26] as well as trifluoromethionine[27] and trifluoroleucine,[23] are translationally active. Such amino acids are readily incorporated into proteins in vivo through the use of auxotrophic bacterial strains. In our continuing effort to understand the effects of fluorination on the structure and function of peptides and proteins, we report herein the influence of trifluoroleucine substitution on the lipid-binding and self-association properties of melittin.

Experimental Section

Materials and General Methods. Wild-type melittin from bee venom (93%, Sigma Chemical Co.) was purified by ion-exchange chromatography,[28] desalted using a Sep-pak C18 cartridge (Waters), and lyophilized to a final purity of >99% by analytical HPLC. N-Fmoc protected l-5,5,5-trifluoroleucine (mixture of the 2*S*,4*S* and 2*S*,4*R* diastereomers) was synthesized according to literature procedures.[24] DOPC was purchased from Avanti Polar Lipids as lyophilized powder, and prepared as a 20 mg/mL stock solution in $CHCl_3$. The buffer for the tetramerization and lipid-binding studies was composed of 10 mM Tris and 1 mM $Na_2EDTA{\cdot}2H_2O$, adjusted to pH 7.5 (Tris buffer). Peptide concentrations were determined by UV spectroscopy using an absorption coefficient of 5570 M^{-1} cm^{-1} at 280 nm.[29] All peptides were prepared as concentrated stock solutions and stored at −20 °C, divided into small portions, which were thawed only once. Fluorescence measurements for the tetramerization and lipid-binding experiments were carried out on a PTI spectrofluorimeter. Emission maxima were obtained by a Gaussian curve-fit of the pseudosymmetrical top portion of the emission peak.

Peptide Synthesis. Three different melittin analogues, with trifluoroleucine replacing Leu9 (M-9tfl), Leu13 (M-13tfl), and all four Leu residues (M-alltfl), were synthesized at the Biopolymer Synthesis Center of the California Institute of Technology. Automated, stepwise synthesis was performed on an ABI 433A synthesizer according to standard Fmoc protocols, using extended coupling cycles for incorporation of the trifluoroleucine residues. After chain assembly, the peptides were deprotected and removed from the resin support with trifluoroacetic acid (TFA) in the presence of 1,2-ethanedithiol, thioanisole, and water, followed by precipitation into cold diethyl ether and isolation via centrifugation. Analytical and preparative HPLC was carried out on a Varian ProStar HPLC system, using a linear gradient from 0.1% aqueous TFA to 60% acetonitrile/0.1% TFA over 30 min. Analytical HPLC of the crude peptides resolved both M-13tfl and M-alltfl into two main fractions with slightly different retention times. In each case the resolved fractions had identical masses, and were thus identified as different diastereomers (M-13tfl) or diastereomeric mixtures (M-alltfl), arising from the unresolved stereocenter at the γ-position of 5,5,5-trifluoroleucine. During purification by preparative HPLC, M-13tfl and M-alltfl were collected as two fractions each, with M-13tfl-A and M-alltfl-A corresponding to the peaks at shorter retention times and M-13tfl-B and M-alltfl-B corresponding to the peaks at longer retention times. For a comparison of retention times, analytical HPLC of pure wild-type (wt) melittin and the five fluorinated analogues was carried out on a Vydac 218TP C18 analytical column (5 μm, 300 Å, 4.6 × 150 mm). Peptides were identified by mass spectrometry, yielding the expected MH^+ monoisotopic masses.

NMR Experiments. NMR samples of M-13tfl-A and M-13tfl-B were prepared to a concentration of 7 mM in CD_3OH and adjusted to an uncorrected glass electrode reading of 5.0. NOESY, TOCSY, and gradient DQF-COSY spectra were recorded at 25 °C on a Varian INOVA 600 MHz spectrometer equipped with a three-axis gradient triple resonance probe. Mixing times of 38 and 350 ms were employed for the TOCSY and NOESY spectra, respectively. Suppression of the methanol OH resonance was accomplished either via presaturation during the relaxation delay (DQF-COSY, TOCSY) or using watergate solvent suppression (NOESY). The spectral width was 8000 Hz in all experiments. The TOCSY and NOESY spectra were recorded with 512

(11) Rex, S.; Schwarz, G. *Biochemistry* **1998**, *2336*, 6−2345.
(12) Pawlak, M.; Stankowski, S.; Schwarz, G. *Biochim. Biophys. Acta* **1991**, *1062*, 94−102.
(13) Rex, S. *Biophys. Chem.* **1995**, *58*, 75−85.
(14) Resnati, G. *Tetrahedron* **1993**, *49*, 9385−9445.
(15) Sheppard, W. A.; Sheetz, C. M. *Organic Fluorine Chemistry*; W. A. Benjamin, Inc.: New York, 1969.
(16) Gough, C. A.; Pearlman, D. A.; Kollman, P. *J. Chem. Phys.* **1993**, *99*, 9103−9110.
(17) Krafft, M. P.; Riess, J. G. *Biochimie* **1998**, *80*, 489−514.
(18) Ringel, I.; Jaeff, D.; Alerhand, S.; Boye, O.; Muzaffar, A.; Brossi, A. *J. Med. Chem.* **1991**, *34*, 3334−3338.
(19) Takagi, Y.; Nakai, K.; Tsuchiya, T.; Takeuchi, T. *J. Med. Chem.* **1996**, *39*, 1582−1588.
(20) Kirk, K. L.; Nie, J. Y. Fluorinated Amino Acids in Nerve Systems. In *Biomedical Frontiers of Fluorine Chemistry*; Ojima, I., McCarthy, J. R., Welch, J. T., Eds.; ACS Symp. Ser. No. 639; American Chemical Society: Washington, DC, 1996; Vol. 639, pp 312−328.
(21) Lo Nostro, P. *Adv. Colloidal Interfacial Sci.* **1995**, *56*, 245−287.
(22) Marsh, E. N. G. *Chem. Biol.* **2000**, *7*, R153−R157.
(23) Tang, Y.; Ghirlanda, G.; Petka, W.; Nakajima, T.; DeGrado, W. F.; Tirrell, D. A. *Angew. Chem., Int. Ed. Engl.* **2001**, *113*, 1542−1544.
(24) Tang, Y.; Ghirlanda, G.; Vaidehi, N.; Kua, J.; Mainz, D. T.; Goddard, W. A., III; DeGrado, W. F.; Tirrell, D. A. *Biochemistry* **2001**, *40*, 2790−2796.
(25) Bilgiçer, B.; Fichera, A.; Krishna Kumar, K. *J. Am. Chem. Soc.* **2001**, *123*, 4393-4399.
(26) Sun, Z. Y.; Pratt, E. A.; Ho, C. ^{19}F-Labeled Amino Acids as Structural and Dynamic Probes in Membrane-Associated Proteins. In *Biomedical Frontiers of Fluorine Chemistry*; Ojima, I., McCarthy, J. R., Welch, J. T., Eds.; ACS Symp. Ser. No. 639; American Chemical Society: Washington, DC, 1996; Vol. 639, pp 296−310.
(27) Duewel, H.; Daub, E.; Robinson, V.; Honek, J. F. *Biochemistry* **1997**, *36*, 3404−3416.
(28) Wille, B. *Anal. Biochem.* **1989**, *178*, 118−120.
(29) Quay, S. C.; Condie, C. C. *Biochemistry* **1983**, *22*, 695−700.

*t*1 × 2k *t*2 complex points, and zero-filled to 2 k *t*1 × 2 k *t*2 complex points for analysis. Squared cosine window functions were applied to the data prior to Fourier transformation and baseline correction.

1D ^{19}F NMR spectra were recorded on a Varian Mercury 300 MHz NMR spectrometer equipped with a 4-nuclei probe. The NMR sample of 5,5,5-trifluoroleucine was prepared to a concentration of 7 mM in CD_3OH. $CFCl_3$ was added as internal standard to all three NMR samples. The spectral width was 50 000 Hz, with 16 k complex points, zero-filled to 64 k complex points for analysis. Exponential multiplication with a line-broadening factor of 1 Hz was applied to the data prior to Fourier transformation.

Vesicle Preparation. For the lipid-binding studies, 3.95 mL of the DOPC stock solution in $CHCl_3$ were placed into a test tube, evaporated to dryness under a stream of nitrogen, and completely dried under high vacuum for 3 h. After rehydration with 5 mL of Tris-buffer and vortexing, the multilamellar vesicle solution was extruded 15 times through two stacked polycarbonate filters of 100 nm pore size, using a Lipex T.004 extrusion system. The final phospholipid concentration was determined to be 20.46 mM, according to the Fiske-Subbarow phosphate assay against suitable standards.[30]

Tetramerization Studies. Titrations were carried out in the presence of 100 and 50 mM Na_2SO_4. In both cases, 80 μL of a 400 μM peptide solution in Tris buffer and 80 μL of Tris buffer containing twice the final concentration of Na_2SO_4 were mixed thoroughly in a 13 × 13 mm quartz fluorescence cuvette, to obtain a final peptide concentration of 200 μM. Spectra were recorded with excitation at 280 nm, an emission scan between 320 and 380 nm, and 2 nm slit widths. Before each subsequent spectrum was acquired, the peptide solution was diluted 2-fold by removing 80 μL of the mixture and replacing it with 80 μL of Tris buffer containing the appropriate amount of Na_2SO_4 , followed by thorough mixing. The emission maxima resulting from two separate titrations per peptide were averaged before data evaluation.

Lipid-Binding Studies. Of a 5 μM peptide solution in Tris buffer, 2 mL were placed into a 1 × 1 cm quartz fluorescence cuvette equipped with a magnetic stir-bar. Spectra were recorded with excitation at 280 nm, an emission scan between 320 and 380 nm, and 2 nm slit widths, at 298 K. Aliquots of the DOPC stock solution were added with constant stirring. An equilibration period of 5−10 min before recording the spectra was found to be necessary for the first few additions, up to a lipid concentration of about 200 μM. To account for scattering by the liposomes, background spectra of DOPC vesicles added to blank buffer were subtracted from the raw data. The emission maxima resulting from two separate titrations per sample were averaged before data evaluation.

Results and Discussion

From the crystal structure of melittin it can be seen that the side chains of Leu9 and Leu13 are oriented approximately orthogonal to the plane defined by the bent helical rod, while those of Leu6 and Leu16 lie within this plane, pointing toward the convex and concave sides, respectively (Figure 1A). We selected Leu9 and Leu13 as the two single-substitution sites. The top view of the dimer forming the asymmetric unit reveals that Leu13 is the only leucine residue that makes van der Waals contact to its equivalent in the second strand of the dimer (Figure 1B), while Leu9 and Leu16 are involved in leucine−leucine contacts between the two dimers forming the tetramer.

Stereochemistry, Hydrophobicity, and Structure. The synthesis of 5,5,5-trifluoroleucine used in this work yields a mixture of the 2*S*,4*R*- and 2*S*,4*S*-diastereomers (Scheme 2). Incorporation of this mixture results in two diastereomers each for the two monosubstituted melittins, and 16 diastereomers for the tetrasubstituted melittin.

The two diastereomers of M-9tfl elute as one peak in standard RP-HPLC. In contrast, HPLC of crude M-13tfl reveals two peaks, one from each of the two diastereomers. The 16 diastereomers for M-alltfl also elute as two peaks, which are consequently isomeric mixtures. Partitioning into the stationary phase of a C18 column is believed to disrupt intermolecular hydrophobic interactions of amphiphilic peptides while retaining their α-helical structure, as shown by circular dichroism spectroscopy (CD) of model peptides adsorbed onto C-18 coated quartz plates.[31] Similarly, the elution buffer (>40% acetonitrile) has been shown to disrupt quarternary, but not secondary interactions, as verified by CD and size exclusion chromatography.[32] RP-HPLC retention times are thus a measure of the hydrophobicity of the helical monomer. In the case of membrane-active peptides, correlation has been observed between lipid-induced helicity and RP-HPLC retention time; amphiphatic peptides that adopt conformations characterized by extended hydrophobic contact areas exhibit retention times longer than those predicted on the basis of amino acid retention coefficients.[31,33] In this study, retention time increases in the order M-13tfl-A < wt < M-9tfl < M-13tfl-B < M-alltfl-A < M-alltfl-B (Figure 2). A significant influence is apparent for the side chain stereochemistry of Leu13, which is located in the hinge region of the bent helical rod. The unusually short retention time of M-13tfl-A suggests a conformational change

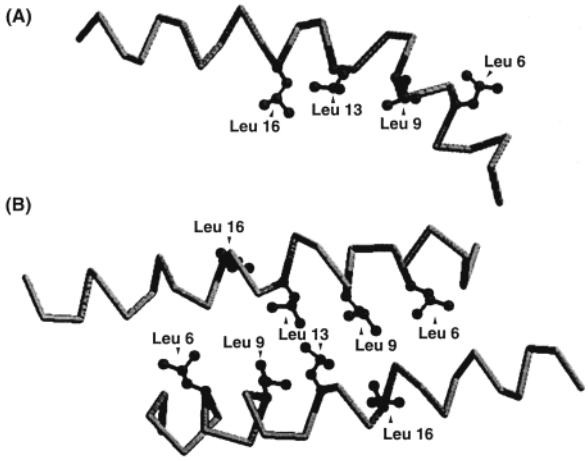

Figure 1. Positioning of the leucine side chains as taken from the crystal structure:[5] (A) side view onto a melittin monomer and (B) top view onto the melittin dimer forming the asymmetric unit.

Scheme 2. Incorporation of 2*S*,4*R*- and 2*S*,4*S*-5,5,5-Trifluoroleucine into Melittin

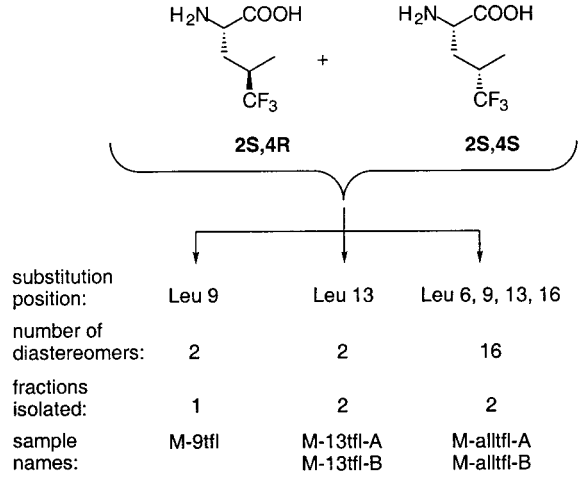

(30) Bartlett, G. R. *J. Biol. Chem.* **1958**, *234*, 466−468.

(31) Blondelle, S. E.; Ostresh, J. M.; Houghten, R. A.; Perezpaya, E. *Biophys. J.* **1995**, *68*, 351−359.

(32) Lau, S. Y. M.; Taneja, A. K.; Hodges, R. S. *J. Chromatogr.* **1984**, *317*, 129−140.

(33) Blondelle, S. E.; Lohner, K.; Aguilar, M. I. *Biochim. Biophys. Acta* **1999**, *1462*, 89−108.

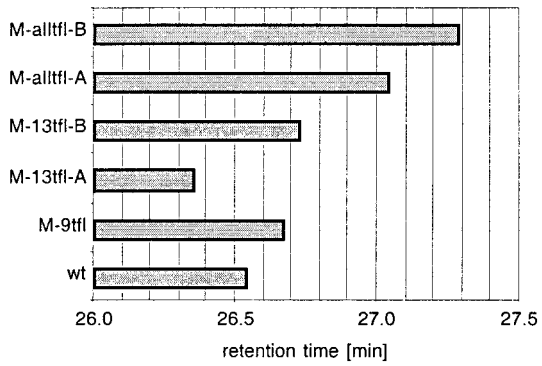

Figure 2. RP-HPLC retention times of wild-type and fluorinated melittins

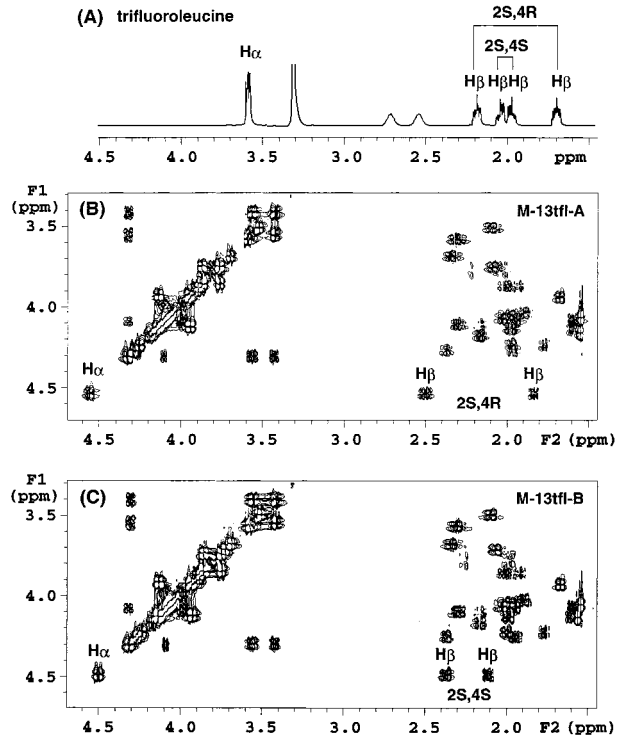

Figure 3. Comparison between the 1D ^{1}H NMR spectrum of the diastereomeric mixture of 2*S*,4*R*- and 2*S*,4*S*-5,5,5-trifluoroleucine (A) and the equivalent region of the DQF-COSY spectra of M-13tfl-A (B) and M-13tfl-B (C) showing the Hα-Hβ cross-peaks.

at the hinge region of the peptide, leading to less favorable alignment of the hydrophobic faces of the bent helical rod. The fact that Leu9 elutes as one peak and that M-alltfl is resolved into just two peaks indicates that not all stereoisomers affect the hydrophobicity in a similar manner.

The stereochemistry of the trifluoroleucine side chain can be assigned via the NMR chemical shifts of the β-hydrogens.[34] Four multiplets are observed for the diastereomeric mixture of the free amino acid, with the inner two corresponding to the β-hydrogens of the 2*S*,4*S*-isomer, and the outer two corresponding to the β-hydrogens of the 2*S*,4*R*-isomer (Figure 3A). We determined the chemical shifts of the trifluoroleucine side chains of M-13tfl-A and M-13tfl-B through a series of 2D-NMR experiments in methanol, in which melittin exists as helical monomer, circumventing the aggregation observed in water.[35] The sequential assignment of the backbone proton resonances

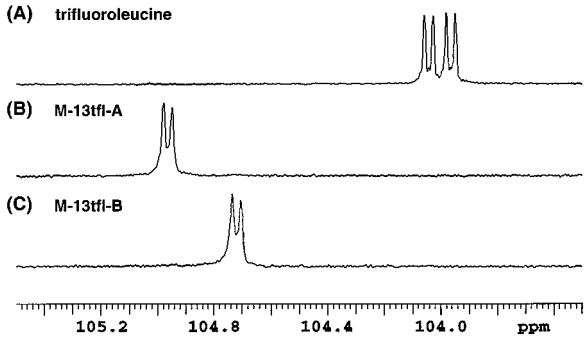

Figure 4. ^{19}F NMR spectra of (A) trifluoroleucine, (B) M-13tfl-A, and (C) M-13tfl-B in CD_3OH.

was possible with only one interruption due to Pro 14, using the NOE connectivities between NH protons of adjacent residues, in combination with the fingerprint region of the DQF-COSY spectra. Several ambiguities due to similar chemical shift values were solved via the TOCSY spectra. From the CH α-CHβ cross-peaks of the DQF-COSY spectra it can be seen that M-13tfl-A and M-13tfl-B correspond to the 2*S*,4*R*- and 2*S*,4*S*-diastereomers, respectively (Figure 3B,C). The downfield shift of the α and β protons compared to those of the free amino acid is expected, due to incorporation of trifluoroleucine into the peptide chain. Further evidence for the diastereomeric purity of M-13tfl-A and M-13tfl-B comes from the ^{19}F NMR spectra, in which just one doublet is observed for each of the two peptides, while a pair of doublets is observed for the diastereomeric mixture of the free amino acid (Figure 4).

The NOESY spectra of M-13tfl-A and M-13tfl-B confirmed the overall helical structure of the fluorinated peptides through a series of intense α_i-NH_{i+3} NOEs. Additionally, most backbone proton chemical shifts of wt melittin, M-13tfl-A, and M-13tfl-B agree to within 0.03 ppm. The only major difference is observed for the Ala15 amide hydrogen of M-13tfl-A, which is shifted downfield by >0.2 ppm, compared to that of wt melittin and M-13tfl-B. Although it is not possible to correlate a single change in chemical shift of an amide proton with a specific change in conformation, this observation is consistent with structural alteration at the Leu13-Pro14-Ala15 hinge region of M-13tfl-A. To investigate further the structural difference between M-13tfl-A and -B we have crystallized the two peptides, and determination of their X-ray structures is currently under way.

Melittin Self-Association. We next investigated the effect of fluorination on melittin tetramerization in aqueous medium of high ionic strength. Upon self-association, Trp19 is removed from the aqueous environment and buried in the hydrophobic interior of the tetramer, resulting in a blue-shift of the emission maximum. From the emission spectra obtained at different peptide concentrations, the fraction of tetrameric melittin (x) can be derived according to

$$x = \frac{(\lambda_M - \lambda)}{(\lambda_M - \lambda_T)} \quad (1)$$

where λ_M and λ_T are the emission maxima of the monomer and tetramer, respectively. As described by Schwarz and Beschiavili,[36] for a simple monomer−tetramer equilibrium the association constant (K_a) and the critical concentration c_p*, i.e., the concentration at which 50% of the peptide is in the aggregated form, can be derived from

(34) Weinges, K.; Kromm, E. *Liebigs Ann. Chem.* **1985**, *1*, 90−102.
(35) Bazzo, R.; Tappini, M. J.; Pastore, A.; Harvey, T. S.; Carver, J. A.; Campbell, I. D. *Eur. J. Biochem.* **1988**, *173*, 139−146.
(36) Schwarz, G.; Beschiavili, G. *Biochemistry* **1988**, *17*, 7826−7831.

$$\frac{x}{(1-x)^4} = 4K_a c_p{}^3 = 8\left(\frac{c_p}{c_p{}^*}\right)^3 \quad (2)$$

where c_p is the total protein concentration. A plot of $\log(x/(1-x))^4$ vs $\log c_p$ is expected to be linear with a slope of 3.

The results obtained for the tetramerization studies show that melittin self-association occurs more readily upon substitution with trifluoroleucine, but that the extent of the observed decrease in c_p* depends on the position into which trifluoroleucine is introduced (Table 1). In all cases, a linear relationship with a slope of approximately 3 was obtained for the double-logarithmic plots (Figure 2), in accord with a simple monomer−tetramer equilibrium. Noteworthy is the difference in self-association between the two diastereomers M-13tfl-A and M-13tfl-B. While the less hydrophobic (2*S*,4*R*) M-13tfl-A displays a c_p* comparable to that of wt melittin, the more hydrophobic (2*S*,4*S*) M-13tfl-B shows a significant decrease, indicative of stronger self-association. In the crystal structure of the wt tetramer, the 4-*pro-S* methyl groups of Leu13 in chains A and C are in van der Waals contact with the 4-*pro-R* methyl groups of Leu13 in chains B and D, respectively. Thus, there is no simple explanation for the observed difference in self-association for M-13tlf-A and M-13tfl-B. X-ray structure determination of M-13tfl-A and -B is expected to provide a better understanding of the difference in self-association exhibited by the two diastereomers.

For M-9tfl an even lower c_p* is observed. Fluorination of all four Leu side chains in the case of M-alltfl-A and -B, however, leads to only a slight further decrease in the value of c_p*, compared to M-9tfl. Although the individual contributions of the trifluoroleucine side chains in positions 6 and 16 of the tetrasubstituted peptide are not known, these two residues appear to have only a minor stabilizing influence. This finding is in agreement with the crystal structure of the wt peptide, which shows the side chains of Leu 9 and 13 to be closely packed at the core of the tetramer. The side chains of Leu 6 and 16, on the other hand, are located near the periphery of the tetramer, less effectively sequestered from the aqueous medium, and with less potential for hydrocarbon−fluorocarbon separation.

Lipid-Binding Behavior. We investigated the effect of fluorination on the affinity of melittin to large unilamellar DOPC vesicles. Under the starting conditions of the assay, i.e., low peptide concentration and low ionic strength, both the wt and the fluorinated melittins exist in aqueous solution as random coil monomers. Addition of DOPC vesicles causes lipid binding of melittin and transfer of Trp19 from the aqueous environment into the hydrophobic interior of the membrane. As in the case of self-association, the resulting blue-shift of the tryptophan emission (Figure 6) can be used to derive the fraction of membrane-bound melittin (ϕ), according to

$$\phi = \frac{(\lambda_f - \lambda)}{(\lambda_f - \lambda_b)} \quad (3)$$

where λ_f and λ_b are the emission maxima of free and membrane-bound melittin, respectively.[37] Melittin binding to lipid membranes is generally described as a partition equilibrium of the peptide between the aqueous and lipid phases. Under ideal conditions, a plot of the ratio of bound peptide per phospholipid vs the concentration of free peptide is expected to be linear, but instead marked curvature is observed (Figure 7). This deviation is a result of repulsive electrostatic interactions between the lipid-bound, positively charged peptide molecules. To account for the nonideal behavior of membrane-bound melittin, the activity coefficient α is introduced into the partition equilibrium

Table 1. Critical Concentrations and Association Constants for Melittin Tetramerization

	100 mM Na_2SO_4			50 mM Na_2SO_4		
	c_p* [μM][a]	K_a [M^{-3}][a]	slope	c_p* [μM][a]	K_a [M^{-3}][a]	slope
wt	14.88	6.07E + 14	3.06			
M-13tfl-A	14.53	6.52E + 14	3.49	31.81	6.21E + 13	3.33
M-13tfl-B	6.81	6.34E + 15	3.37	14.38	6.72E + 14	3.33
M-9tfl	4.29	2.54E + 16	3.29	9.70	2.19E + 15	3.30
M-alltfl-A	3.14	6.49E + 16	3.01	6.01	9.19E + 15	3.02
M-alltfl-B	3.48	4.74E + 16	3.05	5.96	9.45E + 15	3.35

[a] Uncertainties are estimated to be about ±5% for both c_p* and K_a.

$$r = \left(\frac{\Gamma}{\alpha}\right)c_f \quad (4)$$

where Γ represents the water/membrane partition coefficient, r equals c_b/c_l, and c_b, c_f, and c_l are the concentrations of bound and free peptide and phospholipid, respectively.[6] The nonideal behavior of membrane-bound melittin can be treated as a consequence of electrostatic repulsion, and described using the Gouy−Chapman model for charged surfaces, in which the activity coefficient α is a function of the effective charge ν of the membrane-bound peptide.

$$\alpha = e^{2\nu \sinh^{-1}(\nu br)} \quad (5)$$

The dimensionless constant b accounts for geometric factors and salt effects.[6] The two variables Γ and ν can be derived through a nonlinear least-squares curve fit of known values for r and c_f.

Substitution of all four leucine residues with trifluoroleucine results in a significant increase in the membrane affinity of melittin (Figure 7), with a larger effect observed for the more hydrophobic M-alltfl-B than for the less hydrophobic M-alltfl-A. The partition coefficient, which would be expected to correlate with the hydrophobic character of the peptide, increases only approximately 2-fold upon introduction of four trifluoroleucine residues (Table 2). However, fluorination causes a marked decrease in the effective charge ν, even though it is unlikely that fluorination significantly affects the charge of the membrane-bound peptide. In this context, it should be noted that analysis according to eq 4 assumes the peptide in the lipid phase to be monomeric. The equation can be extended to take oligomerization of membrane-bound peptide into account, but the shape of the association isotherm is relatively insensitive to peptide aggregation in the lipid phase. It has been pointed out by Hellmann and Schwarz[38] that it is not possible to extract the aggregation constant from the experimental association isotherm. The same authors have simulated isotherms for systems that exhibit peptide aggregation in the lipid bilayer and subsequently fitted these isotherms to eq 4. Their results show that peptide aggregation leads to an effective charge equal to or smaller than, and a partition coefficient equal to or larger than, the input values. We propose that the decrease in ν observed here for the fluorinated peptides is indicative of peptide aggregation in the lipid bilayer, possibly due to fluorocarbon−hydrocarbon separation.

(37) VanVeen, M.; Georgiou, G. N.; Drake, A. F.; Cherry, R. J. *Biochem. J.* **1995**, *305*, 785−790.

(38) Hellmann, N.; Schwarz, G. *Biochim. Biophys. Acta* **1998**, *1369*, 267−277.

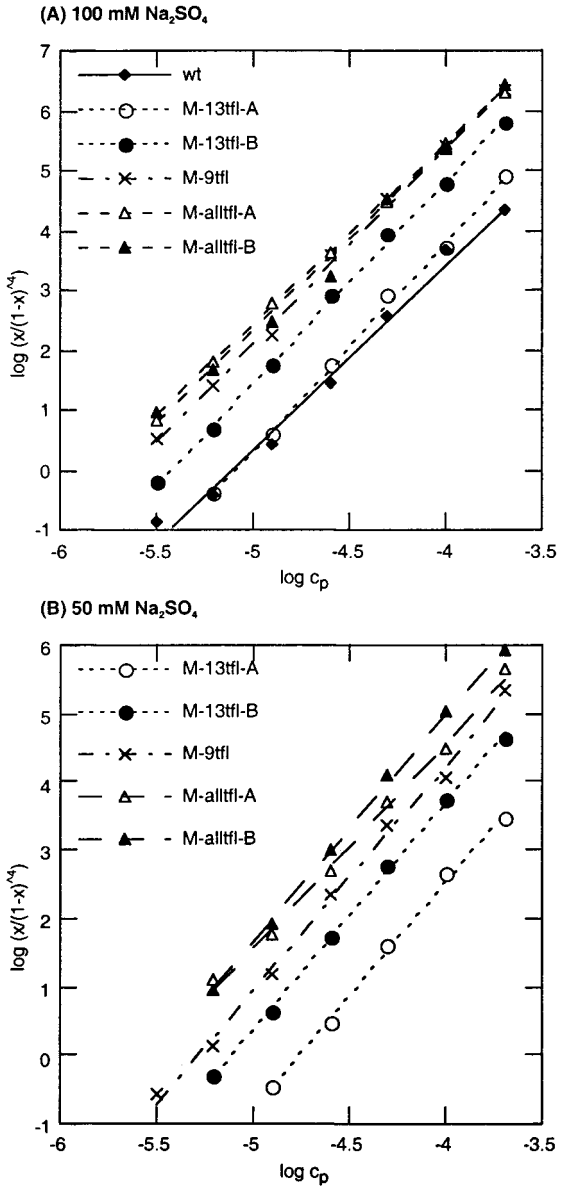

Figure 5. Double-logarithmic plots for the tetramerization equilibria of wild-type (wt) and fluorinated melittins in the presence of (A) 100 mM Na_2SO_4 and (B) 50 mM Na_2SO_4.

The single-site analogue M-9tfl also displays enhanced membrane activity, but to a smaller extent than is observed for the tetrasubstituted analogues. Again a significant difference is observed in the behavior of the two diastereomers M-13tfl-A and M-13tfl-B. The more hydrophobic M-13tfl-B displays enhanced membrane affinity, while the less hydrophobic M-13tfl-A is indistinguishable from wt melittin within experimental error. Comparison of the results obtained for self-association and lipid binding reveals that in both cases the affinity increases in the following order: wt $\approx$ M-13tfl-A < M-13tfl-B < M-9tfl < M-alltfl-A < M-alltfl-B. In the tetramerization studies, the single-site analogues M-13tfl-B and M-9tfl reach about 70 and 90%, respectively, of the effect observed for M-alltfl. The trifluoroleucine residues in positions 9 and 13 of the tetrasubstituted analogues thus account for most of the observed increase in self-association, with little further contribution from Leu 6 and 16. In the case of lipid binding, the increased affinity of M-13tfl-B and M-9tfl is much smaller compared to that of M-alltfl. Again, the individual contributions of trifluoroleucine substitution at positions 6 and 16 are unknown, but these residues clearly are more significant in enhancing membrane affinity than in promoting self-association.

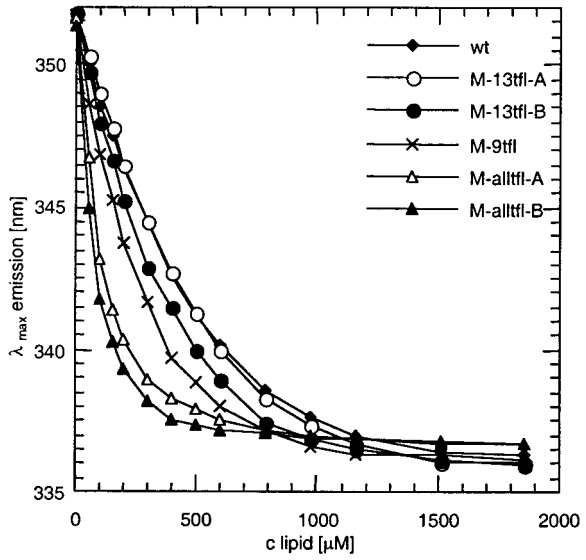

Figure 6. Shift in emission maximum of Trp 19 for wild-type (wt) and fluorinated melittins upon titration of 5 μM peptide in 10 mM Tris, 1 mM EDTA, at pH 7.5 with DOPC LUV's.

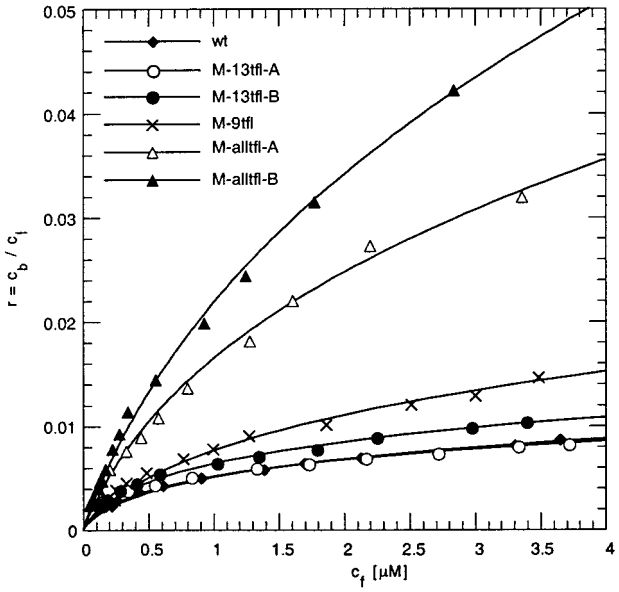

Figure 7. Association isotherms for the binding of wild-type (wt) and fluorinated melittins to the lipid bilayer of DOPC-LUVs.

Table 2. Partition Coefficients and Effective Charges for Melittin Membrane Binding

	Γ [10^4 M^{-1}]	ν
wt	1.69 ± 0.26	1.81 ± 0.08
M-13tfl-A	2.07 ± 0.36	1.94 ± 0.08
M-13tfl-B	2.36 ± 0.28	1.69 ± 0.06
M-9tfl	2.18 ± 0.20	1.34 ± 0.04
M-alltfl-A	3.08 ± 0.30	0.73 ± 0.04
M-alltfl-B	3.53 ± 0.17	0.55 ± 0.02

Conclusions

Incorporation of 5,5,5-trifluoroleucine into melittin increases self-association of the peptide in aqueous medium, and leads to enhanced membrane affinity. If the enhanced membrane affinity were due entirely to increased hydrophobic character

of the fluorinated peptides, fluorination would result in an increased partition coefficient without altering the apparent effective charge of the membrane-bound peptide. Instead, we observe a marked decrease in the apparent effective charge. This observation can be explained as a consequence of melittin aggregation in the lipid bilayer, possibly due to separation of the fluorocarbon side chains of the peptide from the hydrocarbon-rich membrane milieu. Fluorination of peptides and proteins thus presents a strategy not only for control of tertiary and quarternary interactions in aqueous media, but also for enhancement of protein−protein interactions within lipid bilayers. Intramembrane helix−helix association is of central importance in biological processes such as transmembrane signaling and channel formation,[39] and our understanding of the structural basis and the energetics of these interactions is limited.[40] New methods of controlling such interactions would be useful in the de novo design of membrane-bound proteins and peptides with desirable properties.

Acknowledgment. We would like to acknowledge Dr. Suzanna Horvath, Director of the Caltech Biopolymer Synthesis Center, and her staff for synthesis of the melittin peptides and for performing analytical HPLC measurements. We thank Catherine Sarisky and Dr. Scott Ross for help with the 2D NMR experiments. We are grateful to Yi Tang and Dr. Ilya Koltover for helpful discussions and for providing 5,5,5-trifluoroleucine and synthetic intermediates used in these studies. This work was supported by the U.S. Army Research Office and by a gift from the Dow Chemical Company. A.N. thanks the National Institutes of Health for a postdoctoral fellowship.

Supporting Information Available: Tabulated chemical shifts for the backbone and Leu13-side chain proton resonances of M-13tfl-A and -B, and reproductions of the relevant regions of their NOESY and TOCSY spectra (PDF). This material is available free of charge via the Internet at http://pubs.acs.org.

JA004351P

(39) Bormann, B. J.; Engelman, D. M. *Annu. Rev. Biophys. Biomol. Struct.* **1992**, *21*, 223−242.

(40) White, S. H.; Wimley, W. C. *Annu. Rev. Biophys. Biomol. Struct.* **1999**, *28*, 319−365.